Ultrashort-pulse modulation in adiabatically prepared Raman media

Sarah Gundry, Marcel P. Anscombe, Abubaker M. Abdulla, Emiliano Sali, John W. G. Tisch, Paul Kinsler, Geoffrey H. C. New, and Jon P. Marangos

Blackett Laboratory, Imperial College London, Prince Consort Road, South Kensington, London SW7 2BZ, UK

Received July 2, 2004

We demonstrate the efficient modulation of an ~100-femtosecond pulse in a Raman medium coherently prepared by nanosecond pulses. Raman sidebands of the ultrashort pulse spanning 360 THz are generated with an efficiency of >5%. We show that the mechanism permitting the sidebands to be generated is the preparation of a significant vibrational coherence in the medium that is robust to disturbance by an intense short pulse. If the observed sidebands were phase compensated, they would form a short train of approximately ten 3-fs pulses. Focusing would permit the realization of a peak intensity of $>10^{13}$ W cm^{-2}. © 2005 Optical Society of America

OCIS codes: 140.7090, 190.7110.

We report the efficient generation of an ultrabroad spectrum of coherent Raman sidebands by the modulation of a 130-fs pulse in a molecular medium that has been coherently prepared by a pair of nanosecond laser pulses. A number of key advances are demonstrated in this work. We show for the first time to our knowledge that a high-power ultrashort probe pulse can be efficiently modulated in an adiabatically prepared medium, producing a spectrum spanning the range 320–520 nm. The originality lies in the potential to synthesize short trains of, and eventually isolated, few-cycle pulses. The modulator was found to be robust to a probe pulse ten times more intense than the preparation fields. The use of separate nanosecond drive pulses to prepare the sample means that the sideband generation proceeds linearly from the applied short-pulse probe, so detrimental parasitic nonlinear processes are avoided. Finally, since the probe pulse frequency is arbitrary, a broadband field can be generated at any point in the spectrum. For example, using infrared preparation fields, we generated a broadband signal centered at 400 nm.

In earlier work on the adiabatic preparation of gaseous deuterium,[1] Raman sidebands of the fields preparing the modulator spanning an octave of bandwidth were generated. A combination of modulation due to both vibrational and rotational molecular motion was also used to produce more than 100 spectral components.[2,3] The Stanford group recently made progress in reconstructing the phases of multiple Raman sidebands and demonstrated the generation of a train of single-cycle pulses.[4] Although the overall energy conversion efficiency into the Raman sidebands is high in these experiments, the train of pulses produced contains ~10^6 members by virtue of the long pulse duration used. Each pulse in the train is therefore at very low energy compared with that of the driving fields. In contrast, the modulation of an ultrashort pulse in a coherently prepared medium is predicted to produce much shorter trains of higher-intensity pulses.[5] Although the modulation of a low-intensity infrared broadband field in coherently prepared solid hydrogen has been demonstrated,[6] that work cannot be extended to generate short trains of subfemtosecond pulses due to the nanosecond pulse duration.

In our experiment the driving fields preparing the modulator are at 1064.19 nm (Stokes field) and 807.07 nm (pump field). These fields couple the fundamental vibrational transition in D_2 (frequency $\nu_R = 89.81$ THz) with a detuning $\delta(= \nu_P - \nu_S - \nu_R)$ from two-photon resonance that can be varied by tuning pump field frequency ν_p [see Fig. 1(a)]. δ is a critical parameter in the adiabatic preparation process; for the process to be adiabatic a finite detuning is required, although the larger the detuning, the less strongly the fields are able to couple the transition. The sign of δ also determines whether the coherence controlling the modulator oscillates in phase or in antiphase with the driving fields. The Stokes field is produced by a Continuum Powerlite 7010 injection-seeded Nd:YAG laser, outputting 8.5-ns single-longitudinal-mode 80-MHz linewidth pulses with a maximum energy of 200 mJ. The second laser is a Continuum HRL-100Z laser consisting of a tunable optical parametric oscillator and Ti:sapphire-based amplifying stages. This laser produces single-longitudinal-mode 3.5-ns, 200-MHz linewidth pulses with a maximum energy of 10 mJ. The frequency of the tunable pump field is continuously monitored by a Burleigh WA-4500 pulsed wavemeter to a precision of ±25 MHz. Both lasers are loosely focused through the D_2 cell to produce a roughly constant

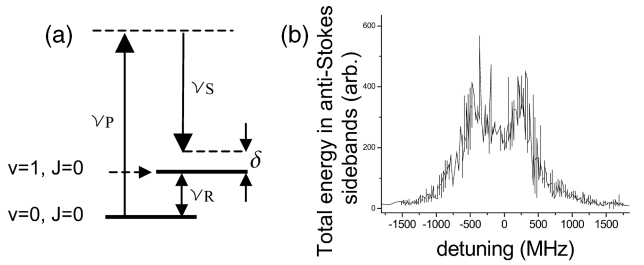

Fig. 1. (a) D_2 energy level scheme. δ shown as positive. (b) Total energy in all anti-Stokes sidebands of driving fields as δ is varied.

0146-9592/05/020180-03$15.00/0

intensity throughout the interaction length of 0.7 and 0.4 GW cm^{-2} for the pump and Stokes fields, respectively. The beam waists of the pump and Stokes fields are 292 and 510 μm, respectively. The D_2 cell is typically kept at pressures of 110–190 Torr at 77 K, cooling being employed both to increase the population in the $(v, J) = (0, 0)$ state and to decrease the Doppler linewidth of the Raman transition.

The probe beam to be modulated by the coherent molecular oscillations induced by the first two lasers is derived from a Ti:sapphire-based chirped-pulse amplifier laser system producing 70-fs pulses with a maximum energy of 40 mJ. A 2-mm-thick KDP crystal is used to frequency double the output of this laser, producing 130-fs pulses at 397 nm with a maximum energy of ~2 mJ. This beam is collimated at a diameter of 2.4 mm and passed through the cell at an intensity of 10 GW cm^{-2}, an intensity nearly 10^3 times greater than that of the probe laser used in previous work,[6] an essential step if high-power subfemtosecond pulses are to be synthesized. All three lasers operate at a repetition rate of 10 Hz and are timed so that the peak of each pulse is coincident in time to an accuracy of ± 0.3 ns. All anti-Stokes sidebands are simultaneously detected with an Ocean Optics USB2000 fiber-coupled spectrometer.

If only the driving fields are applied to the system, 4 orders of anti-Stokes sidebands (AS1–AS4) are observed at the output of the cell when δ is in the range 0–400 MHz below the Raman resonance. At detunings beyond this range, only 1 or 2 orders of anti-Stokes sidebands are observed, and, for detunings greater than 1500 MHz in magnitude, no sidebands are observed. The highest-order measurable sideband (AS4) is found to be brightest at $\delta = -200 \pm 35$ MHz. At this detuning the efficiency with which energy is converted from sideband AS1 to sideband AS4 is maximized and measured at 0.42%. This high value indicates the presence of strong coherence in the sample. The negative value of δ observed to produce the strongest modulation is consistent with measurements made by the Stanford group[1,3] but inconsistent with theoretical analysis.[7] Figure 1(b) shows the δ dependence of the total generated sideband energy. A clear dip is observed at small detunings. This is also characteristic of Raman generation enhanced by coherent adiabatic preparation[1,7] and is attributed to a loss of adiabaticity in this region. Nonadiabatic behavior was experimentally confirmed by observing energy loss in the cell at small δ. We believe our experiment is particularly sensitive to nonadiabatic effects as a result of our relatively large laser linewidth.

The modulation of the 130-fs field at 397 nm is then investigated. The energy of this field injected into the cell is limited to 250 μJ by the damage threshold of the cell windows, corresponding to a peak intensity of 12.5 GW cm^{-2}. At $\delta = -190 \pm 37$ MHz and a D_2 pressure of 150 Torr we observe 2 orders of Stokes (labeled S1 and S2) and anti-Stokes (labeled AS1 and AS2) sidebands of the ultrashort field covering the wavelength range 322–521 nm [Fig. 2(a)]. This detuning corresponds well with the value that generates the maximum number of sidebands of the driving fields. It is important to note that these sidebands are observed only if the driving fields initially prepared the medium. Figure 2(b) shows that, as the probe field intensity varies, the conversion efficiency with which sidebands S1 and AS1 are generated is constant, confirming that the modulator is robust to the presence of the high-intensity probe field.

Figure 3 shows the dependence of the AS1, AS2, and S1 probe field sideband signals on δ. Sidebands AS1, S1, and AS2 are found to be generated with peak efficiencies of $2.5 \pm 0.9\%$ at $\delta = -99 \pm 36$ MHz, $5.0 \pm 1.8\%$ at $\delta = +42 \pm 38$ MHz, and $0.38 \pm 0.19\%$ at $\delta = -190 \pm 37$ MHz, respectively. Since the sidebands shown in this data set were recorded simultaneously, the difference in the values of δ that yield the most efficient generation of different sidebands can be determined to a high accuracy. The maximum total conversion efficiency from the probe field into all sidebands observed is $7.5 \pm 0.9\%$, occurring at $\delta = -13 \pm 38$ MHz. The total conversion efficiency into all sidebands at the detuning found to convert energy most efficiently into the higher-order sidebands (−190 MHz) is found to be $6.1 \pm 0.9\%$.

Figure 4 shows the result of a calculation of the temporal intensity output formed by the interference of all sidebands observed at $\delta = -190$ MHz, assuming

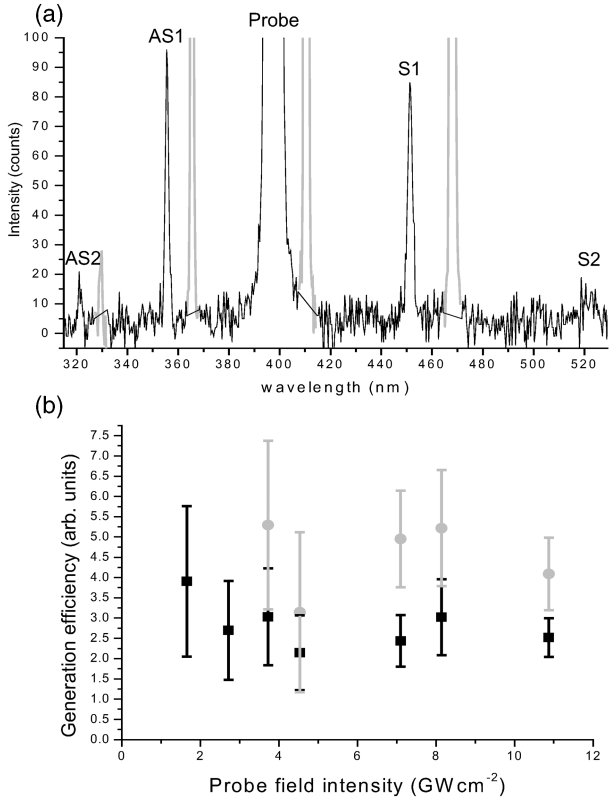

Fig. 2. (a) Spectral output resulting from the propagation of the 130-fs probe pulse through the adiabatically prepared sample at $\delta = -190 \pm 37$ MHz. Sidebands of the probe field are shown in black. Anti-Stokes sidebands of the driving fields (which must also be present if coherent preparation has occurred) are shown in gray. (b) Dependence of the generation efficiency of the probe field sidebands AS1 (black) and S1 (gray) on the intensity of the probe field.

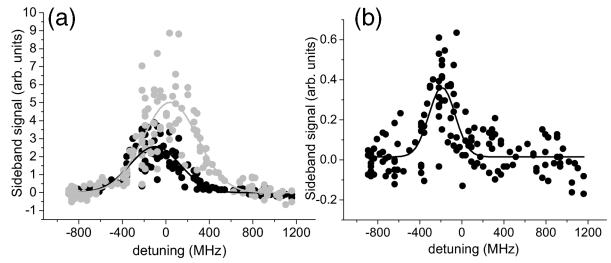

Fig. 3. δ dependence of the probe field sidebands. (a) S1 (gray) and AS1 (black) signals, and (b) AS2 signal (expanded scale). Solid curves show fits to raw data.

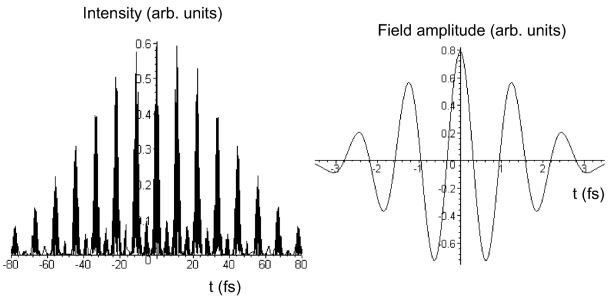

Fig. 4. Calculated train of pulses formed from observed intensity spectra of ultrashort sidebands, assuming constant phase. The electric field amplitude of the central pulse in the train is also shown on an expanded scale.

perfect phase locking. In this calculation the output probe field is attenuated such that its electric field amplitude matches that of the first-order sidebands. A pulse train containing 15 members, each with a duration of 2.8 fs, is generated. After the probe beam is attenuated, the energy within this pulse train is $\sim$0.7 μJ. If focused to a spot size of 10 μm, the peak intensity of each pulse in the train would reach 2.5×10^{13} W cm^{-2}. We note that the UV pulses generated are in the few-cycle domain.

We have conducted simulations of this system in which the molecules are treated as two-level Bloch atoms, and the sidebands are treated as independent fields that are coupled by the Bloch equations. Molecular coupling parameters are determined by comparing the output of simulations to those of experimental small-signal gain measurements. Using our experimental parameters, we find good agreement between the experimental and the predicted output spectra, which yield average conversion efficiencies between the driving field anti-Stokes sidebands of 21 $\pm$ 10% and 18 $\pm$ 4%, respectively, both at $\delta = -200$ MHz. We find from the model that the coherence varies strongly along the interaction length as the strengthening sideband signals affect two-photon Rabi frequency Ω_{PS} in the system but that typical values are 0.12–0.05 at $\delta = 0$ MHz and $\sim$0.005 at $\delta = -200$ MHz. This agrees well with the predicted coherence of 0.004 needed to generate the observed spectrum of the ultrashort pulse.

This relatively low value of off-resonance coherence is due to the steep dependence of the coherence on δ for a system in which Ω_{PS} is relatively low ($\sim$10–20 MHz). However, it should be noted that, even with a coherence of 0.004, strong modulation of the ultrashort field was observed. In our experiment, Ω_{PS} is limited only by the damage threshold of the windows of the cell (20 J cm^{-2}). We are therefore confident that with the simple improvement of lengthening the cell to increase the distance between the windows and the focus of the beams, it will be possible to increase Ω_{PS} to achieve higher values of the off-resonance coherence than were obtained in this experiment. In such a way it is realistic that sidebands of the ultrashort pulse could be generated covering a bandwidth sufficient to support subfemtosecond pulses.

In conclusion, we have shown for the first time to our knowledge that adiabatic coherent preparation at relatively low two-photon Rabi frequencies can be used to produce a coherent molecular oscillation strong enough to efficiently modulate a high-intensity ultrashort field. A bandwidth sufficient to produce a short train of 3-fs pulses easily focusable to intensities of 10^{13} W cm^{-2} has been generated. We expect that with realistic improvements to our system it will be possible to scale up this technique to produce a bandwidth sufficient to generate even higher-intensity subfemtosecond pulses.

S. Gundry's e-mail address is sarah.gundry@imperial.ac.uk.

References

1. A. V. Sokolov, D. R. Walker, D. D. Yavuz, G. Y. Yin, and S. E. Harris, Phys. Rev. Lett. **85,** 562 (2000).
2. M. Katsuragawa, Y. Ono, F. L. Kien, and K. Hakuta, in *Conference on Lasers and Electro-Optics, International Quantum Electronics Conference, and Photonic Applications Systems Technologies Technical Digest on CD-ROM* (Optical Society of America, Washington, D.C., 2004), paper CM06.
3. D. D. Yavuz, D. R. Walker, M. Y. Shverdin, G. Y. Yin, and S. E. Harris, Phys. Rev. Lett. **91,** 233602 (2003).
4. M. Y. Shverdin, D. R. Walker, D. D. Yavuz, G. Y. Yin, and S. E. Harris, in *Conference on Lasers and Electro-Optics (CLEO)*, Postconference Digest, Vol. 96 of OSA Trends in Optics and Photonics Series (Optical Society of America, Washington, D.C., 2004), paper CPDC1.
5. F. L. Kien, N. H. Shon, and K. Hakuta, Phys. Rev. A **64,** 051803(R) (2001).
6. J. Q. Liang, M. Katsuragawa, F. L. Kien, and K. Hakuta, Phys. Rev. Lett. **85,** 2474 (2000).
7. F. L. Kien, J. Q. Liang, M. Katsuragawa, K. Ohtsuki, K. Hakuta, and A. V. Sokolov, Phys. Rev. A **60,** 1562 (1999).